Materiales de Construcción
76 (361) January-March 2026, e398
ISSN-L: 0465-2746, eISSN: 1988-3226
https://doi.org/10.3989/mc.2026.422625

ARTICLE

Optimization of the clinker production process in a Spanish cement factory

Optimización del proceso de producción de clínker en una cementera española

J. Manovel
Department of Mechanical, Informatics and Aerospace Engineering, University of León (León, Spain)
Corresponding author: jmanovel@gmail.com, https://orcid.org/0009-0002-3087-5353

A. I. Fernández-Abia
Department of Mechanical, Informatics and Aerospace Engineering, University of León (León, Spain)
aifera@unileon.es, https://orcid.org/0000-0003-2736-7518

M. A. Castro-Sastre
Department of Mechanical, Informatics and Aerospace Engineering, University of León (León, Spain)
macass@unileon.es, https://orcid.org/0000-0001-5388-2666

Abstract: With the aim of manufacturing a clinker that reduces the energy consumption in its grinding, without substantially modifying the behavior of the cement manufactured with it, a characterization methodology based on the Rietveld method has been developed. From this study we have deduced that one of the most influential factors in the specific consumption of the cement mill is the $C_3S\_M_1$ phase. Therefore, efforts will be focused on promoting its formation in the clinker by controlling the MgO content in the kiln feed and the alumina modulus in the clinker.

Keywords: Clinker; Alite; Rietveld method; DMAIC.

Resumen: Con el objetivo de conseguir fabricar un clínker que permita reducir el consumo energético en su molienda, sin modificar sustancialmente el comportamiento del cemento con él fabricado, se ha desarrollado una metodología de caracterización basada en el método de Rietveld. De este estudio hemos deducido que uno de los factores que más influencia tienen en el consumo específico del molino de cemento es la fase $C_3S\_M_1$, por lo que se va a tratar de potenciar su formación en el clínker controlando el contenido de MgO en la alimentación al horno y el módulo fundente en el clínker.

Palabras clave: Clínker; Alita; Método de Rietveld; DMAIC.

Received: 04-06-2025 / **Accepted**: 12-11-2025 / **Published**: 08-06-2026

Citation: Manovel J, Fernández-Abia AI, Castro-Sastre MA. 2026. Optimization of the clinker production process in a spanish cement factory. *Mater. Construcc*. 76 (361): e398. https://doi.org/10.3989/mc.2026.422625

Supplementary information ↓

1. INTRODUCTION

In the cement industry, Bogue calculations (1) are still widely used to estimate the mineralogical composition of clinker. These calculations are based on X-ray fluorescence (XRF) analysis, which provides the elemental chemical composition of the sample.

Clinker is a highly studied material, and its crystallographic phases have been the subject of much research. In 1887, Henry Le Chatelier (2) observed four different types of crystals when observing clinker under a microscope, and in 1897, Alfred Ellis Törnebohm introduced the terms alite, belite, celite, and felite, the four main crystallographic phases of clinker.

The main component of Portland clinker is tricalcium silicate, $SiO_2(CaO)_3$, abbreviated as C_3S, and its hydration product is the primary source of cement strength (3). The study of this crystallographic phase began in the 1950s when Jeffery determined the crystal structure of pure alite (4). Later, in 1975, Golovastikov obtained the stable crystal structure at room temperature, which is the T_1 form (5). In 2003, De Norfontaine proposed an M_1 model and outlined the relationship between various crystal superstructures, T_1, M_1, and M_3 (6), as showed in Equation [1]:

$$T_1 \overset{620°C}{\longleftrightarrow} T_2 \overset{920°C}{\longleftrightarrow} T_3 \overset{980°C}{\longleftrightarrow} M_1 \overset{990°C}{\longleftrightarrow} M_2 \overset{1060°C}{\longleftrightarrow} M_3 \overset{1070°C}{\longleftrightarrow} R \qquad [1]$$

Where T represents the triclinic form, M the monoclinic form, and R the rhombohedral form.

A widely used method to differentiate between the M_1 and M_3 polymorphs of alite in clinker is the graphical form, which involves focusing on a series of windows or portions of the 2θ scan obtained from the clinker sample being studied (6–9). In industrial clinkers, the difference between M_1 and M_3 polymorphs is evident by looking at the W_3 (31.5-33.5˚ 2θ Cu Kα) and W_5 (51-53˚ 2θ Cu Kα) windows, which have always been considered characteristic of the various alite polymorphs in the literature.

Discriminating between both polymorphs remains a subject of debate and ongoing research, as they significantly influence the subsequent mechanical strength of cement (10). Recent studies have evaluated the statistical validity and variability of several laboratory X-ray diffraction instruments and a synchrotron in determining the concentration of the main crystalline phases of clinker (11). Other investigations focus on the increasing use of alternative fuels due to their environmental and economic benefits in clinker production, as they reduce the reliance on fossil fuels (12).

A substantial body of laboratory-scale research has examined the influence of adding different components on the formation and subsequent stability of various alite polymorphs under specific preparation conditions (3,7,8,13–18). In most of these studies, clinkers were synthesized using analytical grade $CaCO_3$, SiO_2, $Al2O_3$, $Fe2O_3$, and processed in furnaces under controlled pressure and temperature to achieve clinker formation. Additional components commonly found in industrial kilns, particularly sulfur (SO_3) and magnesium (MgO), were often introduced due to their presence in raw materials and fuels used in the process, as they are among the most prevalent minor constituents in industrial clinkers.

To determine whether the transformation into the M_1 polymorph occurs, the MgO and SO_3 content in the clinker plays a crucial role (7,14–17). MgO, when introduced at an optimal range of 2–3 %, lowers the melting temperature, promotes the absorption of free lime and the formation of C_3S (19), and increases the amount of liquid phase during clinker sintering (20). An excessive amount of magnesium oxide, may crystallize as periclase during the cooling stage of the clinker, which can adversely affect cement quality by inducing delayed expansion phenomena (21,22).

SO_3 favors the stabilization of belite and free lime at clinkering temperatures, at the expense of alite content. At high concentrations, SO_3 can lead to alite decomposition, resulting in reduced compressive strength of the final cement (8). It was found that SO_3 can stabilize M_1 alite independently of other foreign ions (23), and it was concluded that gaseous SO_2 may increase the M_1 alite content in sintered Portland cement clinker (24).

High MgO contents promote the formation of small crystals that revert to M_3, while high SO_3 levels favor the formation of larger crystals that tend to transform into M_1. However, the tendency to form M_1 decreases when the alkali-to-SO_3 ratio is high, as SO_3 primarily combines as alkali sulfates. Crystals containing both M_1 and M_3 phases can appear with zoned structures, where M_1 forms the core and M_3 occupies the peripheral regions. This phenomenon occurs because the clinker melt becomes richer in MgO during crystallization, causing the later-deposited material to persist as M_3. The M_3-to-M_1 transformation is also affected by the cooling rate, with slower cooling favoring the formation of M_1. In certain very slowly cooled clinkers, a subsequent transformation to T_2 may occur, although this only happens if the alite contains low levels of substituent elements.

Several studies indicate that the M_1 polymorph exhibits higher mechanical strength than M_3 due to its greater reactivity (8,24). It has been demonstrated that by modifying the MgO/SO_3 ratio, stabilization of M_1 alite could be achieved, resulting in a cement with approximately 10 % higher mechanical strength compared to cement containing M_3 alite (10). Other studies highlight the relationship between the crystal size of C_3S and the strength development of cements at different ages, concluding that crystal size has a more significant influence than the relationship between cement strength and fineness (3,25).

Although considerable efforts have been made to obtain M_1 alite modulated by SO_3 and MgO, few studies have focused on the correlation between the polymorph, alite content in cement clinker, and its mechanical properties (26,27).

All these studies compile a large number of "ideal" scenarios that are very difficult to replicate in an industrial clinker kiln.

At the cement plant involved in this study, powder X-ray diffraction (XRD) combined with the Rietveld method (28) has been used for several years to quantify the crystallographic phases of clinker. For this study, a new analysis program has been implemented—based on a pre-existing one (29)—with the aim of quantifying the two alite polymorphs present in clinker, M_1 and M_3, and investigating whether a relationship exists between the content of these phases and the specific energy consumption of the cement mill. By identifying such a relationship, it may be possible to reduce the energy consumption associated with cement manufacturing by producing a clinker that is easier to grind. This would represent a significant advantage in the current economic climate, characterized by limited civil construction activity and increasingly stringent environmental, CO_2, and energy regulations.

Since the cement mills at the plant are horizontal ball mills, they operate with relatively low energy efficiency and therefore consume a considerable amount of electricity. Optimizing grinding efficiency—specifically by producing a clinker that is more easily grindable—could have a meaningful impact on overall plant operating costs.

2. METHODS AND EQUIPMENT

Over a two-year period, different clinker samples were separated directly from the kiln at specific times and for defined durations. All relevant process data were recorded and stored in a dedicated database to enable independent milling trials with each separated clinker in one of the cement plant's mills.

A total of 52 industrial-scale cement production campaigns were conducted, during which representative samples of the produced cement were collected to monitor the development of its mechanical strength. This was done by casting and testing standardized specimens, as well as conducting other physical and chemical tests as specified in UNE-EN 197-1 (30), to ensure the quality of the cement, since it is intended for commercial use in construction projects.

This study was conducted using the DMAIC methodology, a structured approach aimed at improving existing processes (31). The methodology includes five phases: Define, Measure, Analyze, Improve, and Control, which are detailed below:

The first step, *Define*, involves identifying the nature of the problem in order to establish clear objectives. In this case, the goal was to identify a clinker that is easier to grind, thereby reducing the specific energy consumption of the cement mills.

The second phase, *Measure*, ensures the reliability of the system and the data to be used in subsequent analysis. The results were stored in a shared database specifically created for this purpose, which includes 167 variables. A comprehensive statistical analysis was then performed.

All samples were automatically delivered to the facility's laboratory, the *POLAB AMT* by *Polysius*, where a multi-axis robotic system transported each sample to a disc mill for grinding. The resulting powder was automatically transferred by the robot to a pressing unit, where it was compacted into a 37 mm diameter pressed powder for further analysis.

For elemental analysis, the laboratory is equipped with a *Philips PW2424 Magix* wavelength-dispersive X-ray fluorescence (WDXRF) spectrometer, which provides fast and accurate results.

For crystallographic analysis, a *Philips CubiX Fast X*-ray diffractometer is used, featuring a Bragg-Brentano θ-θ geometry configuration. The instrument scans each sample from 11.6° to 68° 2θ, with a step size of 0.05° 2θ and a dwell time of 30 seconds per step. The X-ray generator operates at 45 kV and 40 mA, providing a detailed diffraction pattern of the sample.

Crystallographic phase quantification of clinker is performed using the *X'Pert HighScore Plus* software, applying the Rietveld refinement method.

To enable automated use of this software in the laboratory, a custom template was developed. This involved manually loading the diffraction pattern of a clinker sample and assigning the target phases using Crystallographic Information Files (CIF) sourced from a free-access database (32). Working ranges for various parameters—such as scale factor, unit cell dimensions, preferred orientation, among others—were defined. After refinement, the resulting fit yielded the following reliability indicators: Rp = 4.68, Rwp = 6.58, and GOF = 5.

The refined template (see Figure 1) serves as a "reference diffraction pattern," allowing weekly recalibration of phase values to standardized starting points, thus enabling the fully automated operation of the software without the need for constant operator supervision.

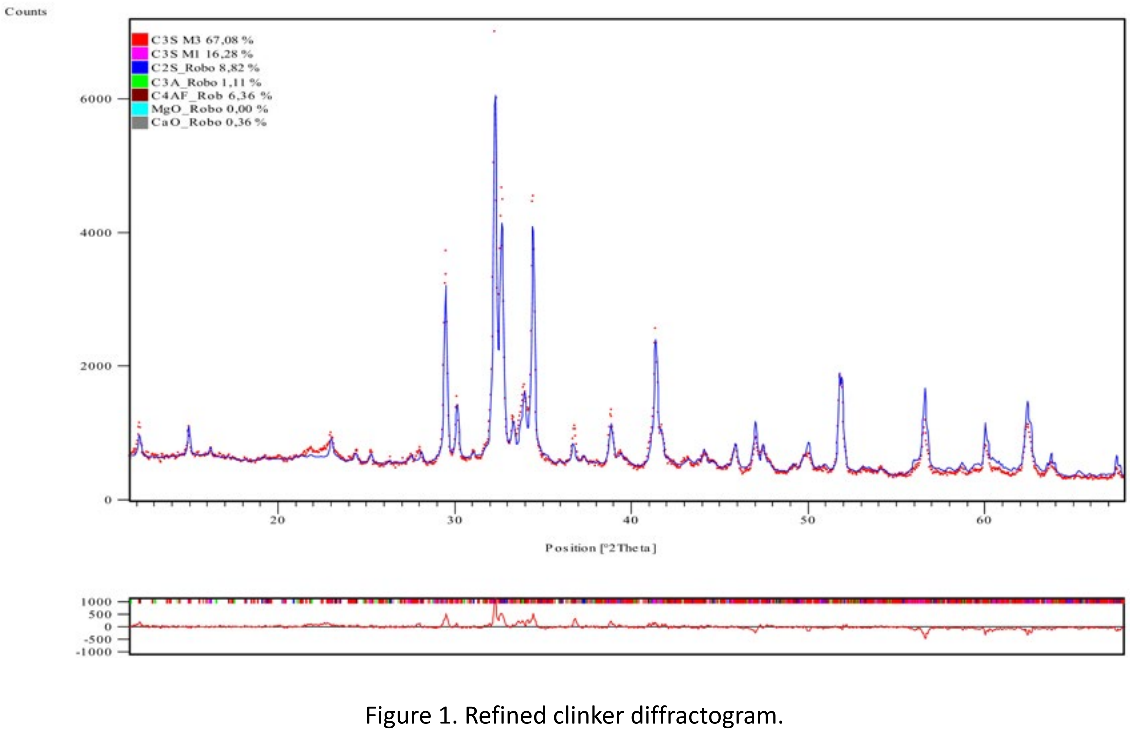

Figure 1. Refined clinker diffractogram.

The crystallographic phases introduced into the analysis software are listed in Table 1:

Table 1. Crystallographic phases.

Crystallographic phase	Label	ICSD Code
Alite M_1	$C_3S\_M_1$	81100
Alite M_3	$C_3S\_M_3$	64759
Belite	C_2S_Beta	81096
Aluminate	C_3A_Cubico	1841
Ferrite	C4AF_IBM2_2003	97926
Free Lime	Cal Libre	61550
MgO	MgO	9863

Subsequently, a custom script was developed to fully automate the Rietveld analysis process within the plant's laboratory. This script automatically transfers all generated results to the central database.

It is important to note that all data collected in this study were recorded at varying time intervals:

- Data recorded every second:
  - Parameters from the preheater-kiln-cooler system (see Figure 2)
  - Parameters from the cement mill (see Figure 3)
- Hourly or bi-hourly laboratory analysis data:
  - Raw meal composition
  - Clinker composition
  - Hot meal composition
  - Cement composition
- Discrete data points:
  - Compressive strength test results from the cement specimens for each of the 52 production trials

All these data were processed to align them as accurately as possible. Hourly averages were calculated for the cement mill and kiln line parameters, and these were correlated with laboratory results from the corresponding cement samples.

The third stage is *Analyze*. In this phase, the objective is to identify the factors that have the greatest impact on process outcomes. A detailed examination of outliers is conducted across all variables, and data points associated with abnormal events—typically related to measurement errors—are removed.

Subsequently, a correlation analysis is performed to determine the strength and direction of the relationships among the variables. For this purpose, a Pearson correlation matrix is used (see Figure 4), which quantifies the linear relationship between the different input (independent) variables included in the model.

To avoid prediction bias, multicollinearity is considered to exist when the absolute value of the correlation coefficient exceeds 0.6 ($|R| > 0.6$), a more conservative threshold than the commonly used $|R| > 0.8$ in other studies (33).

A regression analysis was then carried out using a model that included the variables identified in the previous step, with the aim of determining which ones have the greatest influence on the system. A stepwise regression method was applied, starting with an empty model. Minitab added or removed one variable at each step. The model was considered complete when all remaining variables had p-values greater than the specified *Alpha-to-enter value* (0.1) and less than or equal to the *Alpha-to-remove value* (0.1).

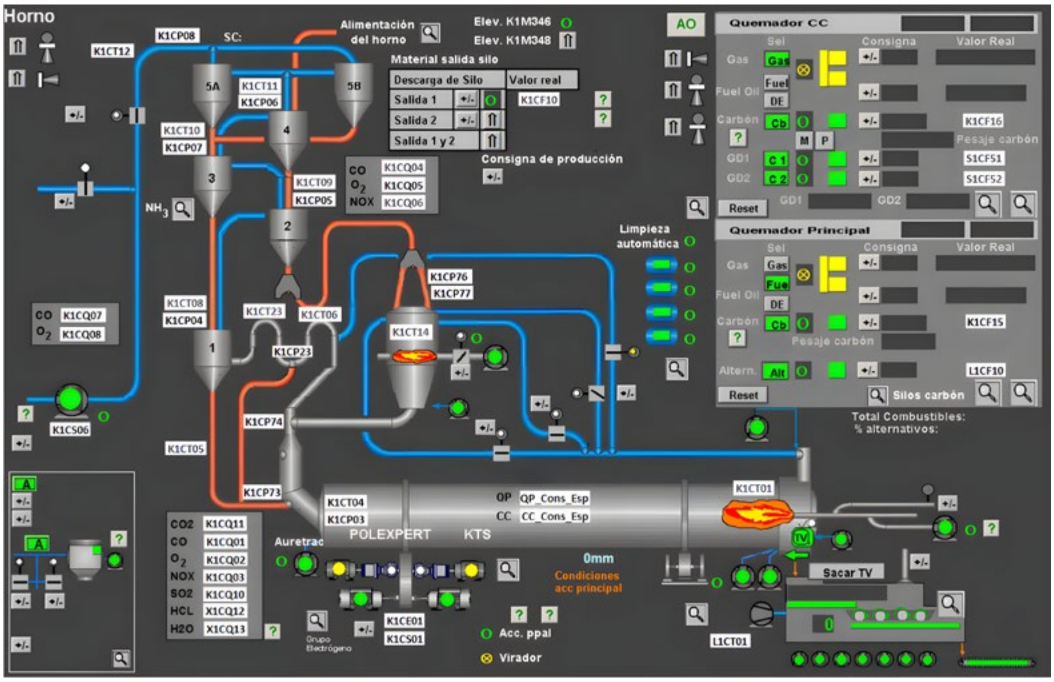

Figure 2. Parameters from the preheater-kiln-cooler system.

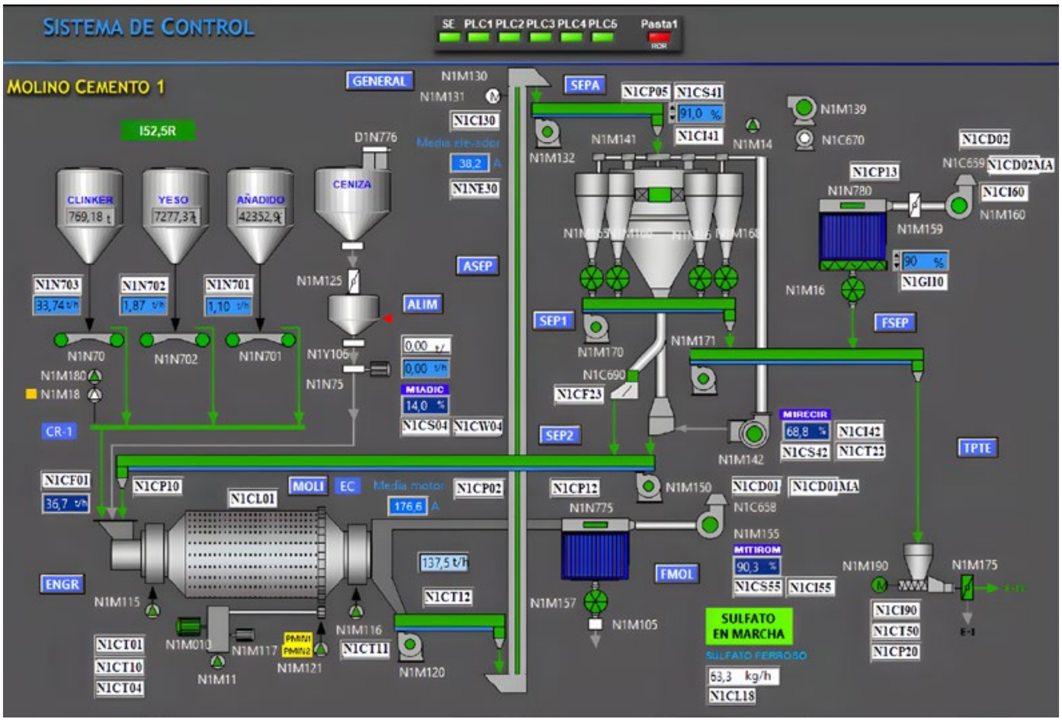

Figure 3. Parameters from the cement mill.

The fourth phase of this methodology is *Improve*, during which several *Design of Experiments (DOE)* were conducted to identify and evaluate the most effective solution for addressing the problem. These experiments involved the controlled production of clinker and cement, where the selected significant variables were varied within their extreme operational ranges. Variables were chosen based on their adjusted sum of squares (Adj SS) obtained from the regression analysis. The effect of these variations on the final output variable was then evaluated.

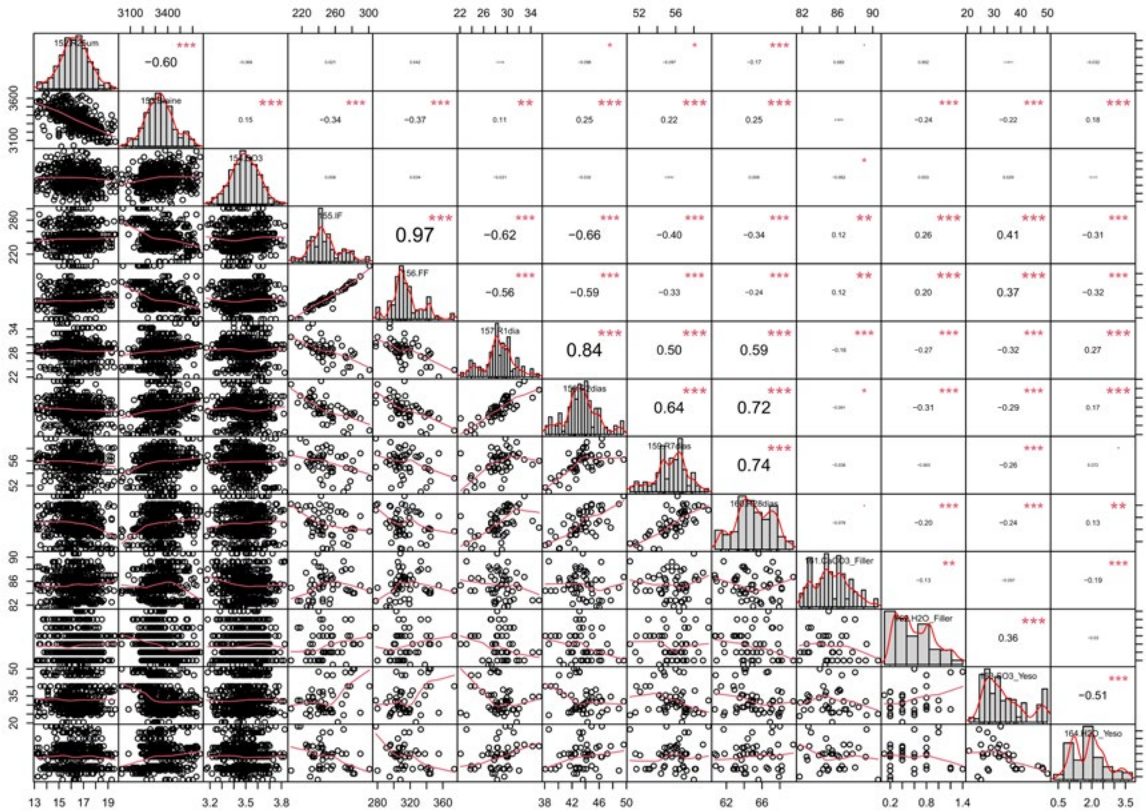

Figure 4. Pearson correlation matrix for cement input variables.

Control is the final and most critical step of the DMAIC methodology. It focuses on consolidating the results and insights gained, and on establishing a framework for continuous improvement. This includes repeating the DMAIC cycle as many times as necessary until no further improvement is possible—indicating that the optimal solution has likely been reached.

3. RESULTS AND DISCUSSION

As previously mentioned, a total of 52 different grinding trials were carried out over a two-year period, amounting to approximately 600 hours of cement mill operation and resulting in the production of around 20,000 tons of cement.

During all these trials, data were collected for 167 variables, which were subsequently used to carry out two linked statistical studies, both following the DMAIC methodology, structured as follows:

3.1. First DMAIC cycle

A study was conducted to identify the variables with the greatest influence on the specific energy consumption of the cement mill. The specific consumption was defined as the output variable. The input variables considered included:

- 33 mill process variables (30 continuous and 3 categorical)
- 7 mineralogical variables obtained via laboratory analysis
- 15 chemical composition variables of the clinker
- 13 chemical and physical parameters of the produced cement

Initially, and after performing an outlier analysis for their removal, a study of potential correlations among the study variables was conducted in order to eliminate those exhibiting strong intercorrelation. For this purpose, several Pearson correlation matrices were developed, Figure 4.

Given the large number of variables considered in this study, the correlation analysis proved particularly useful for reducing the dimensionality of the problem and identifying potential sources of multicollinearity that could compromise the robustness of the predictive models.

Each correlation matrix was independently computed for the three variable blocks: mill operation parameters, clinker characteristics, and cement properties. This approach enabled a more precise analysis within each homogeneous set of parameters. Additionally, it facilitated the comparison of the internal strength of associations within each group and allowed for the formulation of hypotheses regarding how different factors may influence the energy performance of the mill.

After this filtering, the system was reduced to a total of 38 variables, both continuous and categorical, as shown in Table 2.

The continuous variables include those related to the clinker—both its crystallographic characteristics and chemical composition—as well as cement mill process parameters (such as pressures, temperatures, etc.), physicochemical properties of the cement, and the moisture content and carbonate/sulfate proportions of the cement components.

The categorical variables capture the influence of specific energy consumption in relation to the work shift, the season of the year during production, and the operator responsible for the process.

Table 2. Continuous and categorical variables.

Continuous variables			
101.C3S_M1	115.SrO_Clk	129.N1CI42	152.R25um
102.C2S_Rob	116.Cl_Clk	132.N1CI90	154.SO3
103.C3A_Rob	117.MS_Clk	134.N1CP05	158.R2dias
104.C4AF_Rob	118.MF_Clk	138.N1CP20	160.R28dias
110.CaO_Clk	119.SC_Clk	140.N1CS55	161.CaCO3_Filler
111.MgO_Clk	120.Cal_Libre_Clk	141.N1CT04	162.H2O_Filler
112.SO3_Clk	121.PL_Clk	143.N1CT11	163.SO3_Yeso
113.Na2O_Clk	125.N1CD02MA	144.N1CT12	164.H2O_Yeso
114.K2O_Clk	128.N1CI30	147.N1GI10	
Categorical variables			
165.Turno	166.Operador	167.Estacion	

Using the variables listed in Table 2, a stepwise regression method was applied, beginning with an empty model and adding or removing one variable at each step. The model concludes when all variables not included in the model have p-values greater than the specified *Alpha-to-enter* (0.1) and less than or equal to the specified *Alpha-to-remove* (0.1).

Upon completion of the process, the software outputs a model with the following coefficients for the terms that were ultimately retained, as shown in Table 3:

Table 3. Regression model coefficients - DMAIC cement.

Term	Coef	Std error of coef.	T-Value	p-Value	VIF
Constant	18.3	17.2	1.06	0.290	
101.C3S_M1_Rob	- 0.180	0.0164	-11.00	0.000	3.60
103.C3A_Rob	1.100	0.165	6.65	0.000	2.84
110.CaO_Clk	- 1.313	0.289	-4.55	0.000	4.15
111.MgO_Clk	1.700	0.358	4.74	0.000	2.75
112.SO3_Clk	3.452	0.609	5.66	0.000	2.85
114.K2O_Clk	13.64	3.06	4.46	0.000	4.66
118.MF_Clk	- 12.45	2.50	-4.98	0.000	6.67
119.SC_Clk	0.918	0.141	6.53	0.000	3.54
121.PL_Clk	- 0.017	0.0044	-3.81	0.000	2.34
128.N1CI30	0.278	0.0431	6.46	0.000	1.69
132.N1CI90	- 0.152	0.0262	-5.79	0.000	1.58
141.N1CT04	0.043	0.0230	1.86	0.063	4.05
143.N1CT11	- 0.178	0.0236	-7.52	0.000	4.48
144.N1CT12	0.039	0.0207	1.88	0.061	2.10
147.N1GI10	0.010	0.0027	3.89	0.000	1.55
154.SO3	- 1.678	0.481	-3.49	0.001	1.07
158.R2dias	- 0.251	0.0546	-4.60	0.000	6.78
160.R28dias	0.362	0.0501	7.24	0.000	5.16
161.CaCO3_Filler	0.262	0.0479	5.47	0.000	2.59
162.H2O_Filler	0.643	0.230	2.80	0.005	2.04

Where (34):

Coef.: Indicates the relationship between the predictor and the response variable. In the regression equation, the coefficients are the values that multiply the corresponding terms.

Std. Error of Coef.: Represents the standard error of the coefficient, estimating the variability across different estimations of the coefficient.

T-Value: Reflects the ratio between the coefficient and its standard error.

p-Value: This is a probability that measures the evidence against the null hypothesis. A p-value ≤ α is desired. In our case, we use α = 0.1, which indicates a 10% risk of concluding that an association exists when, in fact, it does not.

VIF: The Variance Inflation Factor, $FIV = 1/\left(1 - R_k^2\right)$, where R_k^2 is the coefficient of determination from the auxiliary regression of variable X_k on the remaining explanatory variables. It indicates how much the variance of a coefficient is increased due to multicollinearity among the predictors in the model. VIF values range from 1 to ∞.

It can be observed that none of the p-values exceed the previously mentioned threshold of 0.1; therefore, all variables are considered valid for inclusion in the model.

These coefficients, Table 3, are used to derive the following regression equation (Equation [2]), which represents the resulting model:

$$\text{Specific consumption} = 18{,}3 - 0{,}180\ 101.\text{C3S\_M1} + 1{,}100\ 103.\text{C3A} - 1{,}313\ 110.\text{CaO\_Clk} + 1{,}700\ 111.\text{MgO\_Clk} + 3{,}452\ 112.\text{SO3\_Clk} + 13{,}64\ 114.\text{K2O\_Clk} - 12{,}45\ 118.\text{MF\_Clk} + 0{,}918\ 119.\text{SC\_Clk} - 0{,}017\ 121.\text{PL\_Clk} + 0{,}278\ 128.\text{N1CI30} - 0{,}152\ 132.\text{N1CI90} + 0{,}043\ 141.\text{N1CT04} - 0{,}178\ 143.\text{N1CT11} + 0{,}039\ 144.\text{N1CT12} + 0{,}010\ 147.\text{N1GI10} - 1{,}678\ 154.\text{SO3} - 0{,}251\ 158.\text{R2dias} + 0{,}362\ 160.\text{R28dias} + 0{,}262\ 161.\text{CaCO3\_Filler} + 0{,}643\ 162.\text{H2O\_Filler} \quad [2]$$

Table 4. Model summary - DMAIC cement.

S	R^2	Adj. R^2	Pred. R^2
1.029	70.41 %	68.62 %	65.88 %

Where:

S: Represents the standard deviation of the distance between the fitted and actual values. It indicates how well the model describes the response variable. Lower values suggest a better fit; however, even with a low S, residual plots must be examined to confirm model adequacy.

R-squared (R^2): Represents the percentage of variation in the response variable explained by the model. The higher the R^2, the better the model fits the data.

Adjusted R-squared (Adj. R^2): Indicates the proportion of variation in the response variable explained by the model, adjusted for the number of predictors relative to the number of observations. It is useful for comparing models with different numbers of predictors.

Predicted R-squared (Pred. R^2): Reflects the proportion of variation in the response explained by the model for new (unseen) observations.

Table 4 shows that the model yielded an R^2 of 68.62 % which, while not particularly high, is sufficiently acceptable to proceed with the analysis. At this stage, the main objective is to identify which input variables have the greatest influence on the response variable and over which we may have operational control.

To determine which of the model variables exert the most significant influence on the response variable, an analysis of variance, ANOVA, was requested from the software. The results are shown in Table 5:

Table 5. Analysis of variance. DMAIC cement.

Source	Adj SS	MSE	F Value	p Value
Regression	831.51	41.575	39.26	0.000
101.C3S_M1	128.07	128.075	120.94	0.000
143.N1CT11	59.85	59.853	56.52	0.000
160.R28dias	55.52	55.521	52.43	0.000
103.C3A_Rob	46.90	46.896	44.29	0.000
119.SC_Clk	45.13	45.132	42.62	0.000
128.N1CI30	44.19	44.192	41.73	0.000
132.N1CI90	35.47	35.466	33.49	0.000
112.SO3_Clk	33.98	33.976	32.08	0.000
161.CaCO3_Filler	31.67	31.668	29.90	0.000
118.MF_Clk	26.27	26.267	24.80	0.000
111.MgO_Clk	23.83	23.826	22.50	0.000
158.R2dias	22.40	22.405	21.16	0.000
110.CaO_Clk	21.90	21.896	20.68	0.000
114.K2O_Clk	21.05	21.048	19.88	0.000
147.N1GI10	15.99	15.986	15.10	0.000
121.PL_Clk	15.37	15.365	14.51	0.000
154.SO3	12.91	12.908	12.19	0.001
162.H2O_Filler	8.29	8.285	7.82	0.005
144.N1CT12	3.75	3.753	3.54	0.061
141.N1CT04	3.68	3.676	3.47	0.063
Error	349.46	1.059		
Total	1180.96			

Where:

Adj. SS (Adjusted Sum of Squares): Quantifies the importance and influence of a variable within the regression model. It reflects how much of the total variation is attributed to each predictor, adjusted for the presence of other variables in the model.

MSE (Adjusted Mean Squares): Measures the variability contributed by a specific term in the regression model, assuming all other factors are already included. It is calculated as the adjusted sum of squares divided by the corresponding degrees of freedom.

F-Value: Used to determine whether there are statistically significant differences between the means of two or more groups. In regression analysis, it tests whether a specific predictor significantly improves the model.

p-Value: This is a probability that measures the evidence against the null hypothesis. A p-value $\leq \alpha$ is desired. In our case, we use $\alpha = 0.1$, which indicates a 10% risk of concluding that an association exists when, in fact, it does not.

In the “Adjusted Sum of Squares” (Adj SS) column of Table 5, the importance and influence of each variable within the regression model are quantified. Based on the values in this column, the variable with the greatest influence is $C_3S\_M_1$, which will be used as the output variable in the next step of the study.

As shown in Figure 5, which presents the average specific energy consumption values from each test in relation to the $C_3S\_M_1$ content in the corresponding clinker, it can be observed that when the $C_3S\_M_1$ value exceeds 18 %, a reduction of more than 5 % in the specific energy consumption of the cement mill is achieved. Specifically, the consumption decreases from 39.0 kWh/t to 36.7 kWh/t, resulting in a significant energy saving.

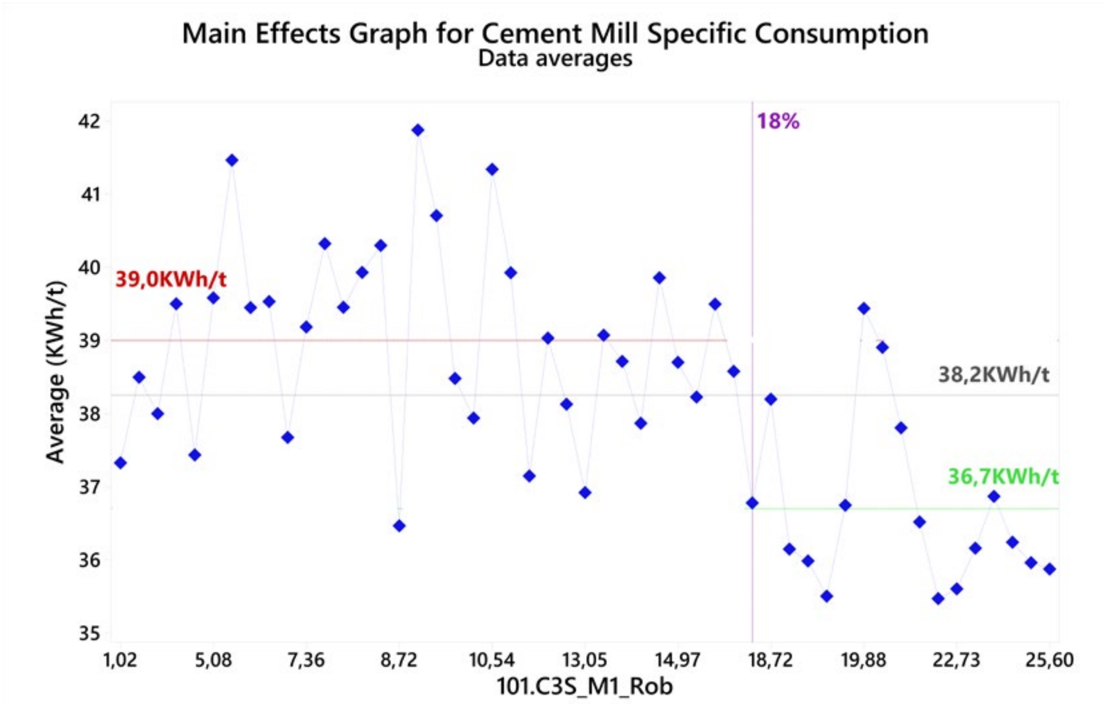

Figure 5. Main effects graph for cement mill specific consumption.

3.2. Second DMAIC cycle

Based on the previous results, which demonstrated that the C_3S_M1 phase has the greatest influence on the specific energy consumption of the cement mill, the objective of this second DMAIC cycle is to identify which variables from the preheater–kiln–feed system most significantly affect the formation of this phase.

Specifically, the analysis includes:

- 56 process variables from the preheater–kiln–feed system
- 42 chemical composition variables provided by the laboratory
- 23 crystallographic characteristics of the clinker and hot meal

As in the first study, an outlier analysis was conducted to remove anomalous values. Subsequently, we examined potential relationships among all variables in order to remove those that were correlated, using Pearson correlation matrices for this purpose. To avoid bias in predictions, a correlation, and hence multicollinearity, was considered to exist between variables when $|R| > 0.6$.

Following this preliminary analysis, a system of 57 continuous variables remained.

Using this refined set of variables, a regression analysis was carried out to identify those with the greatest influence on the system. The same stepwise method employed in the previous case, Section 3.1 – First DMAIC Cycle, was applied. The software then produced a model with the following coefficients for the terms included, Table 6:

Table 6. Regression model coefficients - DMAIC clinker.

Term	Coef	Std error of coef.	T-Value	p-Value	VIF
Constant	112.7	27.9	4.04	0.000	
05.MgO_Alim	-15.807	0.910	-17.36	0.000	6.36
07.K2O_Alim	114.58	8.53	13.43	0.000	6.84
10.Cl_Alim	-1049.5	96.0	-10.93	0.000	6.65
11.MS_Alim	34.97	5.07	6.90	0.000	17.82
12.MF_Alim	-54.85	2.70	-20.28	0.000	7.05
13.SC_Alim	-0.829	0.182	-4.56	0.000	5.44
15.K1CT05	-0.01813	0.00734	-2.47	0.016	3.22
23.K1CT09	-0.11169	0.00824	-13.56	0.000	4.49
24.K1CT10	-0.0596	0.0125	-4.77	0.000	3.38
37.K1CQ02	-0.0821	0.0399	-2.06	0.043	2.61
43.X1CQ13	-0.878	0.197	-4.45	0.000	5.53
44.K1CQ04	-0.2916	0.0985	-2.96	0.004	3.23
47.K1CQ08	-0.472	0.229	-2.06	0.043	4.97
49.K1CS05	0.00865	0.00232	3.73	0.000	2.72
53.C4AF_HC	-4.71	1.26	-3.73	0.000	2.35
62.Mayen_HC	-9.686	0.801	-12.09	0.000	4.85
64.MgO_HC	-6.557	0.491	-13.36	0.000	2.92
73.SO3_HC	-2.459	0.198	-12.44	0.000	5.68
80.K1CT04	0.00298	0.00170	1.76	0.083	3.33
81.L1CT08	-0.01390	0.00270	-5.14	0.000	2.16
82.K1CT01	0.00520	0.00182	2.86	0.005	2.60
93.L1CS11	-1.762	0.313	-5.63	0.000	8.21
96.L1CP56	0.1709	0.0224	7.62	0.000	3.23
112.SO3_Clk	9.39	1.16	8.10	0.000	7.37
114.K2O_Clk	-39.56	4.95	-7.99	0.000	6.99
116.Cl_Clk	24.4	10.7	2.27	0.026	5.26
117.MS_Clk	13.94	3.97	3.51	0.001	14.17
118.MF_Clk	86.43	3.30	26.20	0.000	10.50
120.Cal_Libre_Clk	-9.165	0.944	-9.70	0.000	5.10
121.PL_Clk	-0.02182	0.00659	-3.31	0.001	3.07

As in the first DMAIC, it was observed that none of the p-values exceeded the established threshold of 0.1; therefore, all variables are considered valid for inclusion in the model.

These coefficients, Table 6, are used to derive the following regression equation, which represents the resulting model:

101.C3S_M1_Rob = 112,7 - 15,807 05.MgO_Alim + 114,58 07.K2O_Alim - 1049,5 10.Cl_Alim + 34,97 11.MS_Alim - 54,85 12.MF_Alim - 0,829 13.SC_Alim - 0,01813 15.K1CT05 - 0,11169 23.K1CT09 - 0,0596 24.K1CT10 - 0,0821 37.K1CQ02 - 0,878 43.X1CQ13 - 0,2916 44.K1CQ04 - 0,472 47.K1CQ08 + 0,00865 49.K1CS05 - 4,71 53.C4AF_HC - 9,686 62.Mayen_HC - 6,557 64.MgO_HC - 2,459 73.SO3_HC + 0,00298 80.K1CT04 - 0,01390 81.L1CT08 + 0,00520 82.K1CT01 - 1,762 93.L1CS11 + 0,1709 96.L1CP56 + 9,39 112.SO3_Clk - 39,56 114.K2O_Clk + 24,4 116.Cl_Clk + 13,94 117.MS_Clk + 86,43 118. MF_Clk - 9,165 120.Cal_Libre_Clk - 0,02182 121.PL_Clk [3]

Table 7. Model summary - DMAIC clinker.

S	R^2	Adj. R^2	Pred. R^2
0.674	99.37 %	99.11 %	98.22 %

Table 7 shows that the developed model presents a high goodness of fit, with an R2 of 99.11%, which confirms the model validity. However, as in the first DMAIC cycle, the primary objective is to identify the variables with the greatest influence on the response variable, $C_3S\_M_1$. To this end, an analysis of variance, ANOVA, was performed on the resulting model, and the corresponding results are presented in Table 8.

As with the table obtained in the first study, Table 5, we focus on the second column, Adjusted Sum of Squares (Adj SS), in Table 8 to identify which variables have the greatest influence on the new output variable, $C_3S\_M_1$. From this table, we observe that the most influential variables are the Alumina Module of the clinker (MF_Clk)—defined as the $Al2O_3/Fe_2O_3$ ratio of the clinker—and the MgO content in the feed.

Although the Alumina Module of the feed appears in second position in the table, it is not considered further in this analysis. Despite the model not detecting a direct correlation between the two Alumina modules (clinker and feed), it is known that they are related due to the introduction of end-of-life tires as an alternative fuel in the preheater. These tires contain steel wires that contribute additional iron, affecting the balance.

The residual plots shown in Figure 6 support the validity of the regression model, indicating that the residuals are independent. This is evidenced by the following observations:

- In the normal probability plot of the Figure 6, the points are closely aligned along the reference normal line, indicating that the residuals are approximately normally distributed. This behavior suggests that the model meets the assumption of error normality.
- In the residuals vs. fitted values plot of the Figure 6, shows a random scatter of residuals around the horizontal axis (zero line), with no visible systematic patterns. This indicates that there is no evidence of unmodeled non-linear relationships and that the residual variance remains constant across fitted values, which is desirable. This result reinforces the validity of the model, suggesting that no important variables have been omitted and that the model specification is adequate.
- The histogram of residuals plot of the Figure 6, reveals that the residual distribution is nearly symmetric and centered near zero, with a slight right skew and no notable extreme values.
- In the residuals vs. order plot of the Figure 6, shows no clear systematic trend, such as consistent increases or decreases, indicating independence of residuals over time. Although some noise is present, there is no strong autocorrelation, thereby satisfying the independence assumption.

Table 8. Analysis of variance. DMAIC clinker.

Source	**Adj SS**	**MSE**	**F Value**	**p Value**
Regression	5229.39	174.313	383.32	0.000
118.MF_Clk	312.13	312.126	686.37	0.000
12.MF_Alim	187.02	187.019	411.26	0.000
05.MgO_Alim	137.08	137.081	301.44	0.000
23.K1CT09	83.58	83.577	183.79	0.000
07.K2O_Alim	82.02	82.018	180.36	0.000
64.MgO_HC	81.20	81.197	178.55	0.000
73.SO3_HC	70.36	70.357	154.72	0.000
62.Mayen_HC	66.52	66.517	146.27	0.000
10.Cl_Alim	54.37	54.370	119.56	0.000
120.Cal_Libre	42.83	42.830	94.18	0.000
112.SO3_Clk	29.83	29.827	65.59	0.000
114.K2O_Clk	29.06	29.062	63.91	0.000
96.L1CP56	26.41	26.410	58.08	0.000
11.MS_Alim	21.66	21.664	47.64	0.000
93.L1CS11	14.44	14.438	31.75	0.000
81.L1CT08	12.03	12.030	26.45	0.000
24.K1CT10	10.35	10.345	22.75	0.000
13.SC_Alim	9.45	9.452	20.79	0.000
43.X1CQ13	9.01	9.005	19.80	0.000
53.C4AF_HC	6.34	6.340	13.94	0.000
49.K1CS05	6.33	6.325	13.91	0.000
117.MS_Clk	5.61	5.606	12.33	0.001
121.PL_Clk	4.98	4.981	10.95	0.001
44. K1CQ04	3.99	3.988	8.77	0.004
82. K1CT01	3.73	3.728	8.20	0.005
15.K1CT05	2.77	2.773	6.10	0.016
116.Cl_Clk	2.35	2.350	5.17	0.026
37.K1CQ02	1.93	1.930	4.24	0.043
47.K1CQ08	1.93	1.927	4.24	0.043
80.K1CT04	1.41	1.407	3.09	0.083
Error	33.20	0.455		
Total	5262.59			

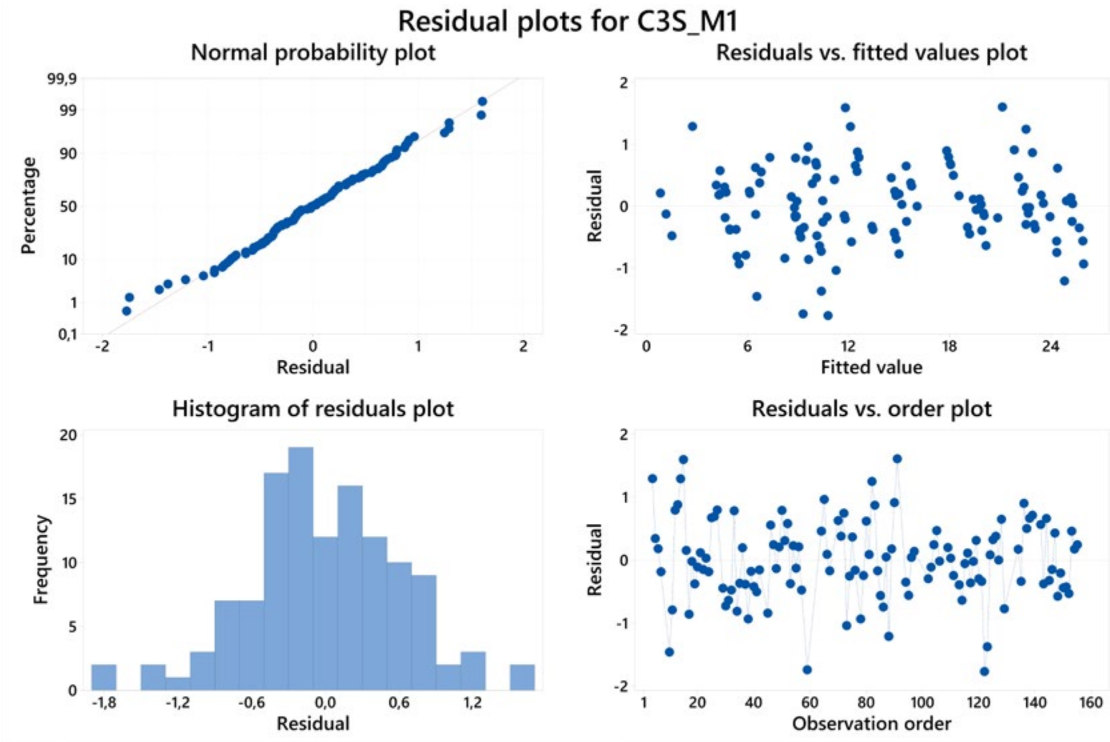

Figure 6. Residual plots for $C_3S\_M_1$.

Once this model was established and the variables with the greatest influence on the $C_3S\_M_1$ phase—and consequently on the specific energy consumption of the cement mill—were identified, a series of Design of Experiments (DOE) was carried out to validate the statistical findings.

4. CONCLUSIONS

From this study, it has been concluded that one of the most influential factors affecting the specific energy consumption of the cement mill is the $C_3S\_M_1$ phase. Therefore, efforts will be made to promote its formation during clinker production.

As shown in Figure 5, when the $C_3S\_M_1$ content is below 18%, the average specific energy consumption is approximately 39.0 kWh/t. In contrast, when the $C_3S\_M_1$ content is above 18%, the average specific consumption decreases to 36.7 kWh/t.

This represents a potential energy saving for the plant and, as a result, this initiative has been included among the Energy Saving Measures adopted by the factory. It will be monitored and controlled both internally and through energy management audits in accordance with UNE-EN ISO 50001:2018 (35).

Since the plant has multiple clinker storage silos, kiln production will be segregated based on the $C_3S\_M_1$ phase content in the clinker. This will allow for continued experimental testing in the future and a more in-depth exploration of this study.

Supplementary information ↑

Funding sources

The authors declare that they have no known financial conflicts of interest or personal relationships that could have influenced the work reported in this article.

Supplementary material

Not applicable.

Data availability

Not applicable.

Acknowledgements

The authors would like to express their gratitude to the company and its employees for their time and dedication, and especially for the patience and support shown by many—particularly the laboratory staff—during the sampling process and execution of the various tests that comprise this study.

Authorship contribution statement

Jesús Manovel: Conceptualization, Data curation, Formal analysis, Investigation, Methodology, Project administration, Resources, Software, Visualization, Writing - original draft.

Ana Isabel Fernández: Supervision, Validation, Writing - review & editing.

María Angeles Castro: Supervision, Validation, Writing - review & editing.

Competing interests

The authors of this article declare that they have no financial, professional or personal conflicts of interest that could have inappropriately influenced this work.

Statement on the use of Artificial Intelligence

Not applicable.

REFERENCES

1. Bogue RH. 1929. Industrial & engineering chemistry analytical edition. Ind Eng Chem Anal Ed.

2. Le Chatelier H. 1887. Recherches expérimentales sur la constitution des mortiers hydrauliques. Paris.

3. Taylor HFW. 2008. Cement chemistry. Chem Eng.:387-433. https://doi.org/10.1142/9781860949982_0010

4. Jeffery JW. 1952. The crystal structure of tricalcium silicate. Acta Crystallogr. 5(1):26-35. https://doi.org/10.1107/s0365110x52000083

5. Golovastikov NI, Matveeva RG, Belov NV. 1975. Crystal structure of the tricalcium silicate $3CaO{\cdot}SiO_2 = C_3S$. Sov Phys Crystallogr.:441-445.

6. Courtial M, de Noirfontaine MN, Dunstetter F, Gasecki G, Signes-Frehel M. 2003. Polymorphism of tricalcium silicate in Portland cement: a fast visual identification of structure and superstructure. Powder Diffr. 18(1):7-15. https://doi.org/10.1154/1.1523079

7. Li X, Xu W, Wang S, Tang M, Shen X. 2014. Effect of SO3 and MgO on Portland cement clinker: formation of clinker phases and alite polymorphism. Constr Build Mater. 58:182-192. https://doi.org/10.1016/j.conbuildmat.2014.02.029

8. Zhou H, et al. 2018. Research on the formation of M1-type alite doped with MgO and SO_3—A route to improve the quality of cement clinker with a high content of MgO. Constr Build Mater. 182:156-166. https://doi.org/10.1016/j.conbuildmat.2018.06.078

9. Bigare M, et al. 1967. Polymorphism of tricalcium silicate and its solid solutions. J Am Ceram Soc. 50(11):609-619.

10. Staněk T, Sulovský P. 2002. The influence of the alite polymorphism on the strength of the Portland cement. Cem Concr Res. 32(7):1169-1175. https://doi.org/10.1016/S0008-8846(02)00756-1

11. Rossetto CM, Carezzatto GL, Martinez LG, Pecchio M, Turrillas X. 2023. Mineralogical analysis of Brazilian Portland cements by the Rietveld method with emphasis on polymorphs M1 and M3 of alite. Bol Soc Esp Ceram Vidr. 62(5):402-417. https://doi.org/10.1016/j.bsecv.2022.06.005

12. Serrano-González K, Reyes-Valdez A, Chowaniec O. 2017. Impact of the use of alternative fuels on clinker reactivity. Mater Constr. 67(326):e120. https://doi.org/10.3989/mc.2017.08215

13. Ludwig HM, Zhang W. 2015. Research review of cement clinker chemistry. Cem Concr Res. 78:24-37. https://doi.org/10.1016/j.cemconres.2015.05.018

14. Uda S, Asakura E, Nagashima M. 2005. Influence of SO_3 on the phase relationship in the system CaO–SiO_2–Al2O_3–Fe_2O_3. J Am Ceram Soc. 81(3):725-729. https://doi.org/10.1111/j.1151-2916.1998.tb02398.x

15. Li X, Huang H, Xu J, Ma S, Shen X. 2012. Statistical research on phase formation and modification of alite polymorphs in cement clinker with SO_3 and MgO. Constr Build Mater. 37:548-555. https://doi.org/10.1016/j.conbuildmat.2012.07.099

16. Gharibi E, Jabri M, Ramdani A. 2017. The effect of magnesium on the alite phase structural stability and its hydration process. J Mater Environ Sci. 8(4):1312-1319. [Internet]. Available from: https://www.jmaterenvironsci.com/Document/vol8/vol8_N4/139-JMES-2932-Jabri.pdf

17. Maki I, Goto K. 1982. Factors influencing the phase constitution of alite. Cem. 12(3):301-308.

18. Her S, et al. 2025. Synthesis and characterization of MgO- and SrO-doped cement: mineralogical composition and polymorphism of cement clinker phases. Constr Build Mater. 487:141994. https://doi.org/10.1016/j.conbuildmat.2025.141994

19. Liu X, Li Y. 2005. Effect of MgO on the composition and properties of alite-sulphoaluminate cement. Cem Concr Res. 35(9):1685-1687. https://doi.org/10.1016/j.cemconres.2004.08.008

20. Altun IA. 1999. Effect of CaF_2 and MgO on sintering of cement clinker. Cem Concr Res. 29(11):1847-1850. https://doi.org/10.1016/S0008-8846(99)00151-9

21. Katyal NK, Ahluwalia SC, Parkash R, Sharma RN. 1998. Rapid estimation of free magnesia in OPC clinker and 3CaO:1SiO_2 system by complexometry. Cem Concr Res. 28(4):481-485.

22. Ren X, Zhang W, Ye J. 2012. Effect of multiple foreign ions doping on hydration reactivity of alite. J Chin Ceram Soc. 40(5):664-670. https://doi.org/10.1016/S0008-8846(98)00027-1

23. Segata M, et al. 2019. The effects of MgO, Na_2O and SO_3 on industrial clinkering process: phase composition, polymorphism, microstructure and hydration using a multidisciplinary approach. Mater Charact. 155:109809. https://doi.org/10.1016/j.matchar.2019.109809

24. Kang R, et al. 2021. The effect of gaseous SO2 secondary sintering on the cement composition and crystal structure. Constr Build Mater. 285:122872. https://doi.org/10.1016/j.conbuildmat.2021.122872

25. Andrade Neto JS, Carvalho IC, Monteiro PJM, Matos PR, Kirchheim AP. 2025. Unveiling the key factors for clinker reactivity and cement performance: a physic-chemical and performance investigation of 40 industrial clinkers. Cem Concr Res. 187:107717. https://doi.org/10.1016/j.cemconres.2024.107717

26. Andrade Neto JS, De la Torre AG, Kirchheim AP. 2021. Effects of sulfates on the hydration of Portland cement – a review. Constr Build Mater. 279:122428. https://doi.org/10.1016/j.conbuildmat.2021.122428

27. Zhou H, et al. 2021. Research on structure modulation of alite and its effect on the mechanical properties of cement clinker. Constr Build Mater. 303:124511. https://doi.org/10.1016/j.conbuildmat.2021.124511

28. Roderick JH. 1993. The Rietveld method. IUCr Monogr Crystallogr. Oxford Univ Press. https://doi.org/10.1107/s0021889894000439

29. Castañón García A. 2011. Optimización del proceso de producción de clínker. Aplicación a la factoría de Tudela Veguín. Univ León. [Internet]. Available from: http://hdl.handle.net/10612/12265

30. AENOR. 2011. Cemento – parte 1: composición, especificaciones y criterios de conformidad de los cementos comunes. UNE-EN 197-1. Madrid.

31. Pande PS, Neuman RP, Cavanagh RR. 2000. The six sigma way. McGraw-Hill Professional Publishing.

32. American Mineralogist Crystal Structure Database. 2026. [Internet]. Available from: https://www.rruff.net/amcsd/

33. Koya BP. 2021. Comparison of different machine learning algorithms to predict mechanical properties of concrete. University of Victoria.

34. Minitab. 2023. Tabla de coeficientes para ajustar modelo de regresión. [Internet]. Available from: https://support.minitab.com/es-mx/minitab/help-and-how-to/statistical-modeling/regression/how-to/fit-regression-model/interpret-the-results/all-statistics-and-graphs/coefficients-table/

35. AENOR. 2018. UNE-EN ISO 50001:2018 sistemas de gestión de la energía. Requisitos con orientación para su uso. Madrid.